Available online at www.sciencedirect.com
SCIENCE DIRECT®
Journal of Molecular Catalysis A: Chemical 220 (2004) 93–102
JOURNAL OF MOLECULAR CATALYSIS A: CHEMICAL
www.elsevier.com/locate/molcata

Novel microstructures and reactivity for *n*-butane oxidation: advances and challenges in vapor phase alkane oxidation catalysis

Kostantinos Kourtakis, Pratibha L. Gai*,[1]

Central Research and Development Laboratories, Experimental Station, DuPont Science and Engineering, P.O. Box 80356, Wilmington, DE 19880-0356, USA

Received 20 January 2004; accepted 3 March 2004

Abstract

The development of novel and improved microstructures is reported for vanadium phosphorus oxide (VPO) catalysts for the oxidation of *n*-butane to maleic anhydride (MA) by grafting alkoxides of bismuth and molybdenum on to pre-formed vanadium phosphorus oxide precursor, $VO(HPO_4)\cdot 0.5\,H_2O$. Depth profiling shows that the surface is molybdenum-rich, following a calcination and activation procedure which converts the catalyst precursor to the final, active phase(s). This novel composition profile in the catalyst may be responsible for the reactivity enhancements observed for this catalyst system. Catalysts prepared using bismuth or molybdenum containing precursors individually do not show a performance enhancement.
© 2004 Elsevier B.V. All rights reserved.

Keywords: *n*-Alkane oxidation; Bi; Mo; V; P; O; Novel microstructures; Grafted catalysts

1. Introduction

The selective oxidation of *n*-butane to maleic anhydride (MA) over vanadium phosphorus oxides (VPO) is an important commercial process [1–12]. Maleic anhydride (MA) is used as a raw material for a variety of products ranging from tetrahydrfurans (THF) to agricultural chemicals. The most successful industrial process to manufacture this compound is the vapor phase oxidation of *n*-butane to MA over active vanadyl pyrophosphate catalysts. In the selective oxidation of the alkane to MA, the most active and selective phase is believed to be vanadyl pyrophosphate, $(VO)_2P_2O_7$ catalysts (hereafter referred to as VPO), with active centers located at the exposed (0 1 0) basal planes [1]. There are also some claims that the active phase is a combination of VPO and VOPO4 phases, or a P-rich phase, or a mixture of VPO with unknown or amorphous phases [1,10]. Direct in situ environmental transmission electron microscopy (ETEM) studies of dynamic butane oxidation over VPO at operating temperatures (∼360–390 °C) have shown the direct evidence of catalyst surface structure modifications leading to glide shear defects and active sites [2]. The studies have shown that anion vacancies are formed following catalyst oxygen loss in butane oxidation and lie in the basal plane between corner-sharing phosphate tetrahedra and vanadyl octahedra. The glide shear defect regions correspond to a slightly anion-deficient defect pyrophosphate phase, with pyrophosphate groups sharing corners similar to metaphosphate $(PO_3)_n$ groups. The local glide defects regions, which maintain the anion vacancies (V^{3+} phases), do not change the overall VPO structure under the catalyst operating conditions and as such are not visible in X-ray diffraction (XRD). In situ ETEM and electron diffraction have thus played a key role in unraveling the catalyst defect structures in butane catalysis.

Several international groups, including ourselves, are working to improve the performance of the catalysts by adding various promoters. A number of cations (e.g. Fe, Cr, Ce, Li, Zn) have been added [6–14] and the literature connected to the promotion of VPO catalysts has been reviewed recently by Hutchings and coworkers [11,14]. However, the surface and bulk microstructural changes of the catalyst due

* Corresponding author. Tel.: +1-302-695-9203; fax: +1-302-695-1664.
E-mail address: pratibha.l.gai@usa.dupont.com (P.L. Gai).
[1] (PL Gai also at: Department of Materials Science, University of Delaware, Newark DE, USA).

1381-1169/$ – see front matter © 2004 Elsevier B.V. All rights reserved.
doi:10.1016/j.molcata.2004.03.053

to promoters, and their effects on the catalytic reactivity are not well understood. It is crucial, therefore, to elucidate the interplay between the promoted structures and reactivity to obtain a deeper understanding of the role of promoted microstructures in alkane oxidation catalysis.

Here we describe microstructures and chemical compositions of promoted VPO catalysts for butane oxidation catalysis. In this study, we investigate alternate synthetic pathways for promoting vanadium phosphates, in order to improve the catalysts further. To understand the observed catalytic improvements, we also investigate the important relationships between the catalyst microstructure and reactor performance for a number of promoted vanadyl pyrophosphate catalysts. Our goal is to obtain insights into the performance improvements observed for these new catalyst systems to guide further design efforts. To understand the complex interactions of VPO with the cation promoters and their effect on reactivity our studies have focused on the bismuth and molybdenum promoted vanadyl pyrophosphates using advanced electron microscopy, X-ray methods and parallel reaction chemistry, which are described in the following sections.

In addition to Bi and Mo, we have prepared other novel compositions using promoter cations. Our approach has been: (1) to substitute a lower valent cation such as Fe^{3+} or, Cr^{3+} for V^{4+}, or (2) to replace V^{4+} with an equimolar combination of cations of different valencies such as Fe^{3+} and Sb^{5+} or bismuth and molybdenum. We have also prepared cerium oxide additions to the VPO catalyst to explore the properties of the promoter as an oxygen reservoir in the alkane oxidation process. In this paper, we discuss our novel finding in the bismuth–molybdenum promoted VPO catalyst system. VPO is orthorhombic with $a = 1.659$ nm, $b = 0.776$ nm and $c = 0.9588$ nm [15]. VPO is a layered structure and the basal (0 1 0) plane, considered to be the active plane, consists of edge sharing pairs of distorted vanadium octahedra shared at corners by the phosphate tetrahedral groups (Fig. 1).

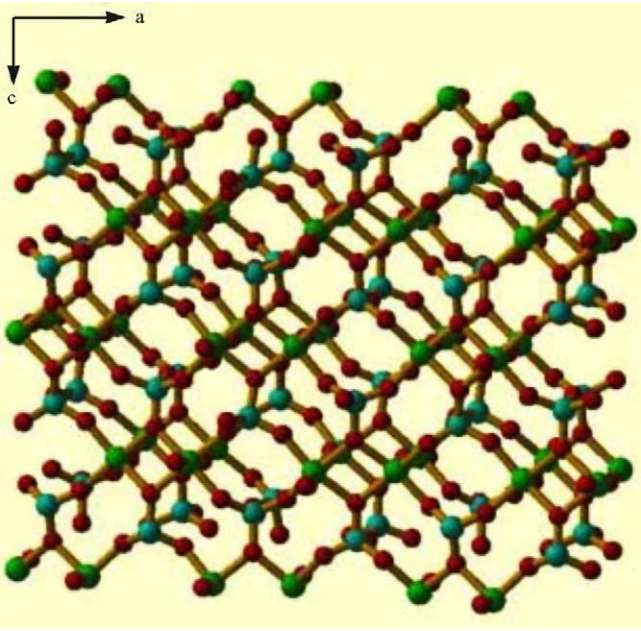

Fig. 1. 3D structural model of VPO catalyst along [0 1 0] with edge-shared vanadyl octahedra interconnected by phosphate tetrahedra.

2. Experimental procedures

2.1. Catalyst synthesis and characterization

A variation of an organic method was employed to synthesize the "base" catalyst precursors [6,16]. Vanadium pentoxide and anhydrous phosphoric acid, prepared by mixing P_2O_5 with aqueous phosphoric acid, are refluxed in 11:1 isobutyl alcohol/benzyl alcohol solvent mixtures under an inert atmosphere. Enough anhydrous phosphoric acid to satisfy a 1.1/1, *P*/*V* atomic ratio is slowly added to the alcohol mixture over a period of 2 h. The solution is allowed to reflux an additional 15 h. Soluble pentavalent vandyl species are reduced predominantly by benzyl alcohol to precipitate the blue tetravalent precursor, which in the case of pure VPO catalysts, crystallizes as $VO(HPO_4)\cdot 0.5\ H_2O$. Excess phosphoric acid is washed from the blue filter cake with fresh isobutyl alcohol. The precursors were subsequently dried under vacuum at 150 °C for 18 h.

To create the novel grafted promoted vanadium phosphate catalyst, a mixture of bismuth and molybdenum alkoxide was used with vanadium hydrogen phosphate hemihydrate precursor. The alkoxides were prepared using bismuth and molybdenum chloride; when reacted with ethanol, they form a soluble mixed alkoxide complex. The bismuth alkoxide is insoluble in the absence of the molybdenum species, suggesting that a soluble alcohol complex has formed containing both bismuth and molybdenum. The mixed alkoxide, dissolved in alcohol, can be reactively grafted onto the pre-formed vanadium phosphate precursor. The catalysts in these experiments contain only 1 mol% bismuth and molybdenum supported on $VOHPO_4\cdot 0.5\ H_2O$. This process is a grafting procedure, since it is likely that the alkoxides of bismuth and molybdenum are reacting with the hemihydrate of the precursor or the hydroxyl groups associated with the hydrogen phosphate, thereby forming covalent linkages of the alkoxy species with the vanadium hydrogen phosphate. This precursor complex is then heated to transform the precursor to the final, promoted catalyst. Calcinations were performed in a small, 3.5 cm fluidized bed on 60 g catalyst samples. Samples were heated in air at 390 °C for 1 h, followed by 460 °C for 18 h in 1.5% butane/air. The relatively high temperature of 460 °C was used for these calcination to for the rapid equilibration of the catalysts.

Powder X-ray diffraction was carried out on the samples. Vanadium oxidation state measurements, as determined by redox titrimetry show small changes in vanadium oxidation state after activation. Likewise, large changes in N_2/BET

surface area are not observed for these systems, suggesting that the increased *n*-butane oxidation activity is due to modification of active sites or an increase in the site density (sites/m^2) of the catalyst surface.

To directly probe the catalyst microstructure, morphology and composition, novel electron microscopy instrumentation and techniques, developed by ourselves, have been used. These include, the pioneering development of in situ atomic resolution- environmental transmission electron microscopy (in situ ETEM) by Gai and co-workers to probe gas–catalyst reactions directly at the atomic scale to provide the dynamic atomic structural information and chemical evolution in catalysts under working conditions [17,18,20,21]. A modified CM30 (S)TEM was used for our in situ ETEM studies of catalysts under controlled reaction conditions to yield a deeper understanding of active sites, transient states and reaction mechanisms which could be directly related to structure-activity relationships in practical reactors.

In the in situ ETEM studies, appropriate gas compositions are used using a conventional reactor-type gas-manifold system, which enables the inlet of flowing gases into the in situ ETEM microreactor. A mass spectrometer is added for gas analysis. Compositions of gases (e.g. 1.5% butane/air) in an in situ ETEM microreactor are comparable to those in a reactor. A sample stage with a furnace allows samples to be heated in the in situ ETEM. Lower gas pressures are used for high resolution imaging. Higher gas pressures are possible with some loss of resolution due to multiple scattering of electrons through gas layers. Experiments on a large number of catalysts [9] have shown that the gas layer in immediate contact with the catalyst surface is the most critical to the catalytic reaction compared to the total amount of gas present. We have used careful conditions in electron microscopy to ensure that the material is not damaged in the electron beam [9]. These include the use of very low dose electron beam currents for imaging materials. The image signal is then amplified by a low light television camera connected to a video monitor, or recorded on a charge couple device (CCD) camera. Calibration 'blank' experiments (without the electron beam) are carried out with the beam switched on for a few seconds only, to record the image and checked with in situ data. Under these careful conditions, no invasive beam damage is observed. Parallel chemical reaction experiments are performed in a microreactor on larger amounts of samples.

In addition high resolution TEM, scanning TEM (STEM) with electron diffraction and electron stimulated energy dispersive X-ray spectroscopy (EDX) for chemical analysis were carried out using a high resolution CM 200 field emission (FE)–(S)TEM system operating at 200 keV, using low electron beam currents. Surface topography of catalysts was investigated using a high resolution low voltage SEM (LVSEM) using an advanced Hitachi SP5000 [19]. The (S)TEM and the SEM systems were fitted with energy dispersive X-ray spectrometers (EDX) and were used for composition analyses of the catalysts. For electron microscopy, catalysts were deposited on 3 mm carbon-filmed copper or titanium microscope grids.

Both as-prepared powders, and cross-sectioned samples were used for compositional depth profile in the samples. First, we carried out analyses from the surfaces of the as-prepared powders, by performing experiments at different electron accelerating voltages in the LVSEM, from the same regions to understand the differences in their surface and bulk composition. The data were confirmed by analyses on cross-sectioned samples; the catalyst particles were cross sectioned to have access to the surface and to the interior (core). EDX compositional analyses, from the surface of cross-sectioned catalyst particles were then repeated at high resolution in the STEM using electron nanoprobes. The electron nanoprobe was moved gradually from the surface to the core of the particle. Analysis spectra were recorded from several dozen particles. The spectra were calibrated using well-characterized Bi_2MoO_6 standards [9] and quantified. The analyses provide high spatial resolution and increased chemical sensitivity, uniquely, from localized regions and the extent of penetration of the promoters into the bulk of the catalyst and the microstructure across the catalyst.

The microstructures were correlated with parallel reaction chemistry in a microreactor. Using these techniques, we elucidate the structure and chemistry of modified catalysts, the nature of catalyst–adsorbate interactions and their role in catalytic selectivity. The synthetic techniques described here have also been applied to robotic synthetic methods and combinatorial tools, in which a number of promoted vanadium phosphorus oxides can be prepared in a parallel manner to cover a broad, promoter composition [22].

2.2. Microreactor evaluations

A fixed bed microreactor was used for catalytic evaluations. The microreactor consisted of a 40.64 cm by 0.64 cm stainless steel tube enclosed by an aluminum sheath (3.12 cm thick, to assist in minimizing thermal gradients) which itself was enclosed in a tube furnace. The reactor was mounted vertically with the direction of the gas flow from top to bottom. Pressure gauges were mounted near both the entrance and exit of the reactor to monitor pressure changes. A bypass valve installed near the reactor entrance allowed the entering gas stream to pass through either the reactor or to bypass the reactor and pass directly to the sampling valve system, allowing analysis of the reactor feed gases prior to reaction. Also, a T-connection at the top of the reactor allowed a thermocouple to be mounted such that it monitored the temperature at the entrance to the packed catalyst bed. Commercially available mass flowmeters (Tylan Model FC-260) of ranges 0–100 and 0–10 cc/min respectively, were used at the reactor feed. The heated exit gas stream (200 °C) passed through a heated sampling valve allowing the selection of a gas sample (250 μl) of the stream for analysis by gas-liquid chromatography (GLC), using commercially available in-

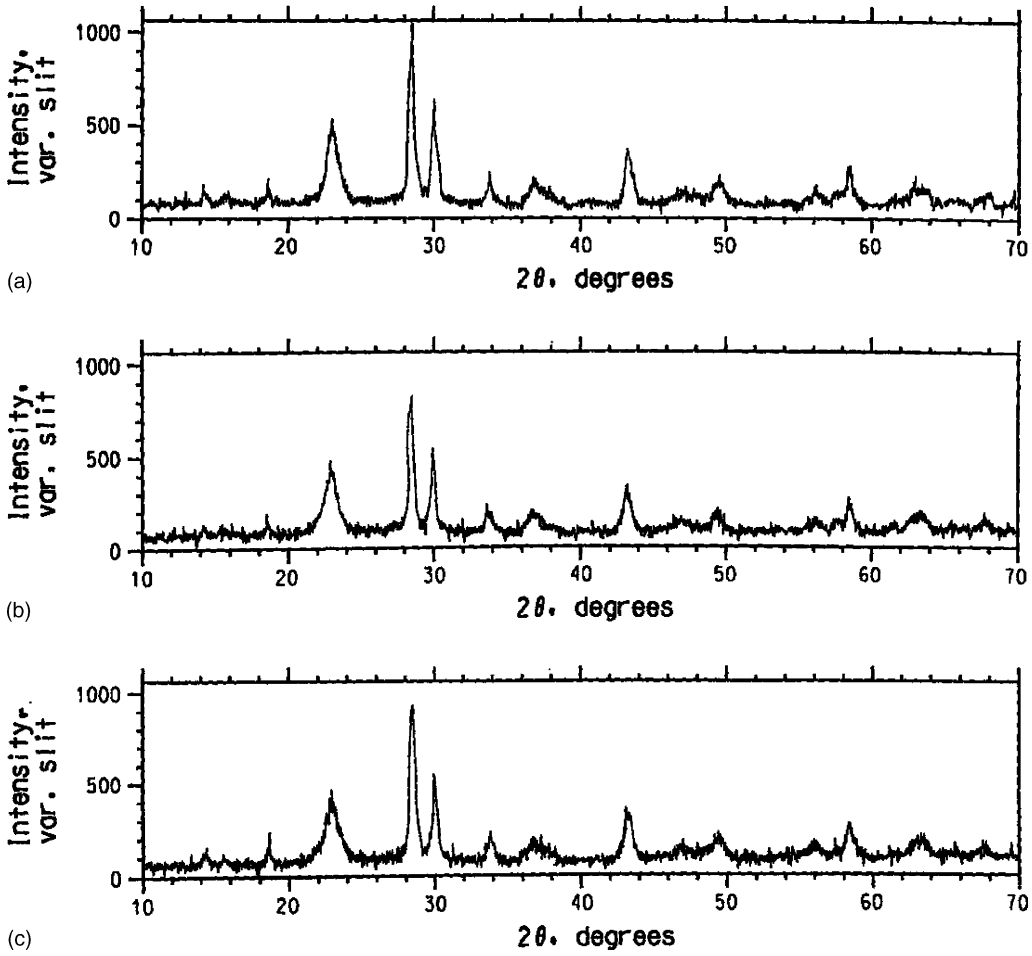

Fig. 2. XRD patterns (following calcination and activation in 1.5% butane/air at 460 °C), for 3 catalysts: (a) Calsicat vanadium hydrogen phosphate precursor with 1 mol% alkoxide solution derived from bismuth trichloride and molybdenum pentachloride; (b) VPO catalyst with ethanol alone; (c) control VPO catalyst. (Peaks, e.g. 020 and 402 are at 2θ (degrees) of $\sim$ 23 and 28.2, respectively).

struments (Gow-Mac Series 740P FID GLC). The GLC was used to analyze for butane and for reaction products, e.g. maleic anhydride, acetic acid, and acrylic acid.

The pseudo first order rate constant k, given for the disappearance of butane, is obtained by fitting the reactor data to a classical first order rate expression:

$$\frac{\mathrm{d[butane]}}{\mathrm{d}t} = -k[\mathrm{butane}]$$

$$\frac{\mathrm{d}(x_0 - x)}{\mathrm{d}t} = -k(x_0 - x)$$

where x_0 is the initial concentration of butane, x the portion of butane reacted.

Integrating this expression gives the concentration of butane exiting the reactor as a function of contact time t, in the reactor:

$$[\mathrm{exit\,butane}] = x_0 - x = x_0 \exp(-kt)$$

In addition to describing the reaction rate of butane with a catalyst, the rate constant k, includes several other factors including the dependence of the reaction rate on oxygen concentration (which remains relatively constant under our conditions) and the concentration of catalyst active sites (also assumed constant).

3. Results and discussion

Powder X-ray diffraction data of Bi,Mo promoted catalysts, catalysts with ethanol alone and control catalysts are shown are shown in Fig. 2a–c, respectively. These diffractograms show single phase crystalline vanadium pyrophosphate. Surface area and redox titrimetry data are listed in Table 1. Table 2 shows data for higher butane concentrations.

As described in subsequent sections, improved reactor performance is observed for the grafted promoted VPO systems. Detailed analysis is also described of the catalyst microstructure using high resolution depth profiling, and this unusual catalyst microstructure which is evolved may be related to improved reactor performance. The results have

Table 1
Fixed Bed Microreactor Data in 2% butane/air, 380 °C, of grafted catalyst systems compared to control catalysts

Catalyst composition	k (s^{-1})	Selectivity at 40% conversion	Vox	N_2/BET SA(m^2/g)
(A) 1 mol% Bi,Mo $VO(HPO_4)\cdot 0.5\ H_2O$	1.02	86	4.07/4.06	34
(B) 1 mol% Bi,Mo $VO(HPO_4)\cdot 0.5\ H_2O$ (duplicate)	0.88	83		
(C) EtOH on $VO(HPO_4)\cdot 0.5\ H_2O$ (control), precursor before activation	0.56	88	4.07/4.05	26
(D) HCl + EtOH on $VO(HPO_4)\cdot 0.5\ H_2O$ (control), precursor before activation	0.49	83		
(E) $VO(HPO_4)\cdot 0.5\ H_2O$ (control), precursor before activation	0.56	86	4.00/4.01	30

been compared with data from the co-precipitated promoter catalyst.

3.1. Microreactor evaluations in 2% butane/air

3.1.1. 1 mol% Bi, 1 mol% Mo supported on pre-formed VPO precursor and comparisons

The catalyst systems described earlier (i.e. catalyst A) in Table 1 was prepared by reactive grafting of the mixed alkoxides of bismuth on molybdenum on pre-formed vanadium hydrogen phosphate precursor followed by calcination and activation at 460 °C in 1.5% butane/air. In Table 1, fixed bed microreactor data obtained using a 2% butane/air feed mixture are shown. The catalyst activity of the catalysts grafted with 1 mol% of bismuth and molybdenum, after the calcination and activation heat treatments in 1.5% butane/air, is shown for catalysts (A) and (B). Remarkably, we find that the pseudo first order rate constant is approximately 60–80% greater than that of the untreated, control catalyst (catalyst E). Catalysts (C) and (D) are additional catalysts which were prepared to determine the effects of solvent (ethanol, for catalyst C) and aqueous hydrochloric acid (catalyst D), on the performance of the pre-formed precursor which is subsequently calcined and activated. This comparison is especially important since some HCl is released during the synthesis of the bismuth/molybdenum alkoxide complex, and the grafting experiments are performed in ethanol. For these treated catalysts (D) and (E), the performance was not improved compared to the control catalyst, (E). N_2/BET surface area measurements show nearly negligible changes in surface area, indicating that the performance improvements of the grafted systems are most likely related to an increase in the density of active sites on the catalyst.

The bismuth/molybdenum grafted catalysts show no change in selectivity to maleic anhydride at 40% conversion, when these catalysts are evaluated in an oxygen rich, 2% butane/air mixture. Aqueous based precursor systems, derived from dissolving bismuth nitrate and ammonium molybdate in water followed by a similar impregnation procedure onto pre-formed vanadium phosphate precursor, do not improve the catalyst.

A series of catalysts were prepared to determine the effect of Bi/Mo ratio and loading on these catalyst systems. As before, each catalyst system is subjected to a calcination and activation heating procedure in 1.5% butane/air prior to reactor evaluations. In this series of experiments, reactor data in 2% butane/air and 9% butane/10% O_2 are tabulated. For

Table 2
Fixed bed microreactor reactor, 2% butane/air, 9% butane/air at 380 °C

Catalyst	2% Butane/air		9% Butane, 10%O_2	
	k (s^{-1})	Selectivity at 40% conversion	Yield	Selectivity
(1) Control catalyst ($VOHPO_4\cdot 0.5\ H_2O$, subsequent to calcination/activation to form the $(VO)_2P_2O_7$ crystalline phase))	0.50	80	7.2	80
(2) 5BiMo (5 mol% Bi, 5 mol% Mo on VPO precursor (on $VOHPO_4\cdot 0.5\ H_2O$))	0.89	66	6.2	60
(3) 1BiMo (1 mol% Bi, 1 mol% Mo on VPO precursor (on $VOHPO_4\cdot 0.5\ H_2O$))	1.12	87	10	70
(4) Higher Bi (5.537 mol% Bi 0.35 mol% Mo on VPO precursor (on $VOHPO_4\cdot 0.5\ H_2O$))	1.84	62	12.8	75
(5) Higher Bi (9.788 mol% Bi, 0.492 mol% Mo on VPO precursor (on $VOHPO_4\cdot 0.5\ H_2O$)); highest Bi/Mo ratio possible using anhydrous chloride alkoxides in EtOH	1.22	71	7.6	71
(6) Higher Mo (5 mol% Bi, 10 mol% Mo on VPO precursor (on $VOHPO_4\cdot 0.5\ H_2O$))	0.92	63	7.4	65
(7) Mo only (1 mol% Mo on VPO precursor (on $VOHPO_4\cdot 0.5\ H_2O$))	0.91	90	9.2	75
(8) 5 mol% Mo on VPO precursor (on $VOHPO_4\cdot 0.5\ H_2O$)	1.22	71	7.6	60

the more reducing, "oxygen lean" gas feed stoichiometries (9% butane/10% O_2), the yield and selectivity to maleic anhydride at that condition is tabulated.

An analysis of these results shows very interesting and remarkable trends which relate to the performance of these catalysts in hydrocarbon lean conditions (2% butane/air) and the hydrocarbon rich, less oxidizing (9% butane, 10% O_2) conditions. Catalysts grafted with molybdenum alone at 1 and 5 mol% concentrations (catalysts (7) and (8)) show improvements in reactivity compared to the control catalyst (1) in 2% butane/air. The addition of bismuth to the 1 mol% composition, as shown in catalyst (3), further improves catalyst performance in 2% butane/air (two-fold increase in activity). Bismuth rich compositions, as exemplified in catalyst (4), show even larger (four-fold) improvements in reactivity, but at the expense of selectivity at 40% conversion in 2% butane/air. Perhaps most interesting however, is the performance in 9% butane/10% O_2. Under reducing conditions, a significant increase in activity is observed and is accompanied by only a small decrease in selectivity. This increase in activity, at high selectivities, in the more reducing environments of 9% butane/air is greater than that observed for the equimolar Bi,Mo composition in catalyst (3) or catalyst (2).

Other trends in this reactor data indicate that increasing the catalyst loading from 1 mol% Bi, 1 mol% Mo (catalyst (3)) to 5 mol% Bi, 5 mol% Mo (catalyst (2)) is not beneficial. A general decrease in maleic anhydride selectivity is observed with increasing levels of bismuth and molybdenum for this catalyst both in 2% butane/air and 9% butane/10% O_2.

To summarize, microreactor data taken over 20 h of exposure to the reaction stream suggests that in the more oxidizing environments (2% butane/air), an equimolar combination of bismuth and molybdenum is preferred. In a hydrocarbon rich environment, however (9% butane/10% O_2), a composition rich in bismuth, in our case with a Bi/Mo ratio of roughly 16, is preferred (catalyst (4) in Table 2). In either case, bismuth is a significantly beneficial co-catalyst, and together with molybdenum, greatly enhances catalyst activity while maintaining a high selectivity to maleic anhydride. Bismuth may function to stabilize molybdenum (or vanadium) in a more stable and selective oxidation state, and this role may become more important under the more reducing conditions of the 9% butane/10% O_2 reactant stream.

3.2. Microchemical investigations: depth profiling

3.2.1. Comparison between grafted and co-precipitated Bi,Mo-promoted VPO catalysts

Important relationships between the catalyst microstructure and reactor performance are being investigated for promoted vanadyl pyrophosphate catalysts. An understanding of these performance improvements observed for these new catalyst systems will help guide further catalyst design efforts.

In depth profiling experiments, a comparison was made between a catalyst formed by the grafting techniques described in the preceding paragraphs and those formed by co-precipitating bismuth and molybdenum precursors with the vanadium hydrogen phosphate precursors during the organic reflux. As shown in Table 1, performance improvements have been observed for the grafted systems in 2% butane/air.

The synthesized catalysts were examined in both plan view and in cross-section. The chemical analyses have shown the presence of a primary phase, $(V_{0.9}\ Bi_{0.05}\ Mo_{0.05}\ O)_2\ P_2O_7$. The presence of this phase has been demonstrated by ETEM structural analyses at the atomic scale and by EDX spectroscopic composition analyses on the nanometer scale, calibrated with Bi_2MoO_6 standards (gamma Bi_2MoO_6). The phase represents a new composition isostructural with vanadyl pyrophosphate. Figs. 3–5 show microstructural morphology, ordered crystal lattice and chemical composition, respectively. Microstructural morphology and microcrystallinity of the grafted (1 mol% Bi,Mo)VPO catalyst are shown in Figs. 3 and 4, respectively. The overlapping microcrystals, all of them showing lattice fringes, are clearly seen Fig. 4. The presence of microcrystals is confirmed by the selected area electron diffraction, which is inset in Fig. 4. Overlapping crystals can create the so-called Moire' fringes [23]. Fig. 5 shows an EDX chemical spectrum from a general area of the catalyst, with the smaller Bi and Mo promoter peaks in VPO. They are magnified in the inset.

The 1 mol% (Bi,Mo)VPO catalysts (catalyst A in Table 1) generally contain variable size (i.e. diameter, or extent across) ranges of plate-like catalyst crystals: many small catalyst particles in the size range 50−150 nm and larger particles upto 0.5−0.7 μm (Fig. 3). Cross-sectional samples and tilting experiments of crystals in the LVSEM were employed to establish crystal (plate) thicknesses. The compositions of the surface and the interiors of the catalyst

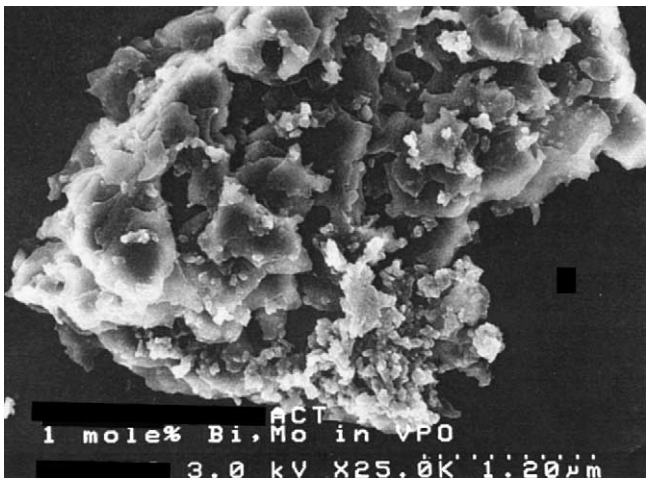

Fig. 3. Microstructural morphology of our novel, grafted 1 mol% (Bi,Mo) promoted-VPO catalysts using LVSEM. Catalysts contain crystals of variable sizes, from 50 to 150 nm upto 0.5 μm.

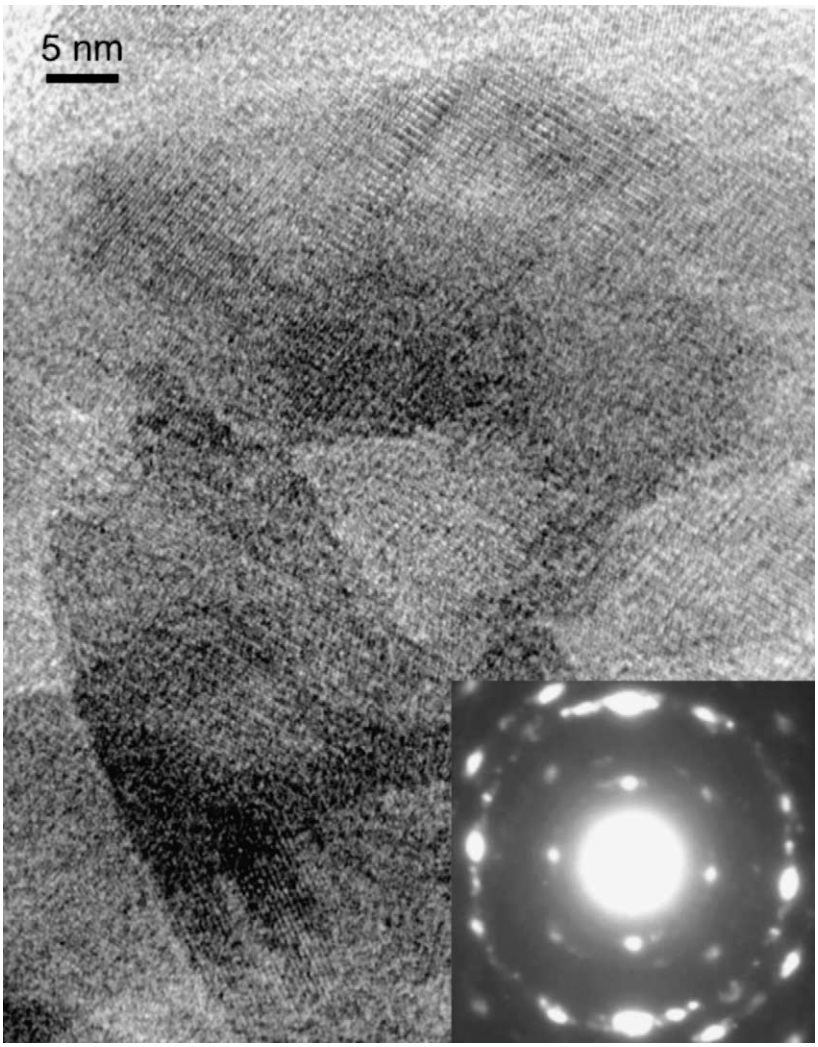

Fig. 4. Atomic resolution environmntal transmission electron microscopy (ETEM) image at room temperature (RT), showing a well ordered grafted 1 mol% (Bi,Mo) promoted-VPO. Crystalline nature of the 1 mol% (Bi,Mo)-promoted catalyst: The microcrystals are in the active (0 1 0) orientation and are aligned randomly with respect to each other. The associated electron diffraction pattern (inset) confirms microcrystallinity.

particles were probed with a view to establishing the extent of penetration or depth of Mo and Bi species into the interior of the catalyst particles and concentrations of the promoters in the VPO structure were estimated.

The precursor alkoxides, originally on the surface of the vanadium phosphate precursor, decompose during the calcination and activation procedure and diffuse from the surface to the catalyst core. Essentially, no secondary phases are observed in the promoted catalyst phase, either by high resolution electron microscopy, or by powder X-ray diffraction. However, detailed compositional depth profiling and microchemical analysis reveal the final catalyst composition is not completely homogeneous in bismuth and molybdenum. Indeed, these studies show that the catalyst surface layers are molybdenum rich and the core of the catalyst particles are enriched in bismuth, in the 1 mol% (Bi,Mo)VPO catalyst. Fig. 6 shows compositional depth profile of Mo/Bi, plotted (with a scaling factor) as a function of depth in the catalyst crystal, from the surface to the center (interior) of the particles. Statistical errors for each data point in the plot are as follows: in the depth, ±0.4 nm and in the Mo/Bi ratios of about ±0.15. Plot A, shows the composition depth profile for the grafted catalyst 1 mol% (Bi,Mo)VPO and plot B, is that for co-precipitated ($Bi_{0.05}$ $Mo_{0.05}$)VPO. Fig. 7 shows the compositional depth profile of Mo/V, confirming the surface enrichment of Mo.

These changes in the depth profile distribution of catalyst composition are not accompanied by changes in surface area, as measured by N_2/BET. The presence of the Mo-rich phase may, therefore be significant and responsible for the observed enhanced catalytic activity, by altering the nature or introducing new active sites on the catalyst surface. As described previously in [2], anion vacancies and glide defects are introduced in VPO following catalyst oxygen loss in butane oxidation, leading to V^{3+} phases. We believe that in the proposed global stoichiometric compound, $(V_{0.9}{}^{4-\delta}$

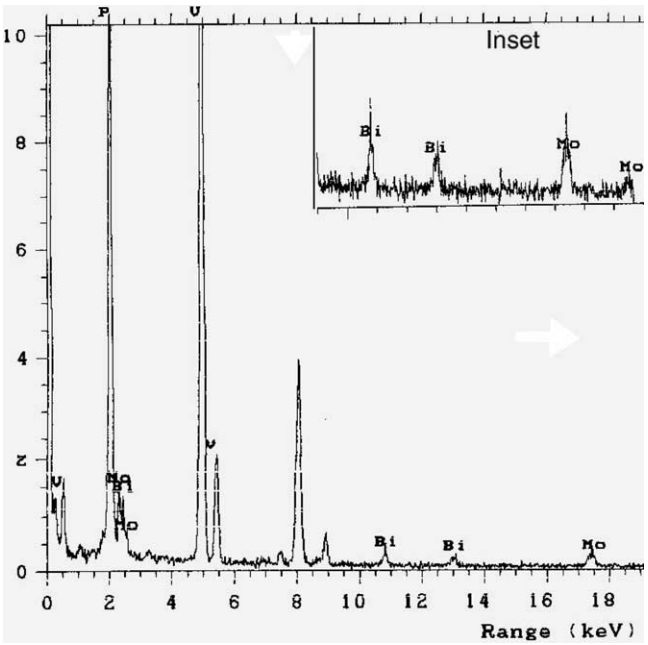

Fig. 5. Compositional spectrum of 1 mol% (Bi,Mo)VPO, using electron stimulated, energy dispersive X-ray spectroscopy (EDX) in the electron microscope. High precision compositional analyses at the nanoscale (using electron nanoprobes) from several dozen crystals away from bars of the grid supporting the sample and various catalyst regions have shown Bi and Mo to be in solid solution with VPO, forming the promoted VPO catalysts.

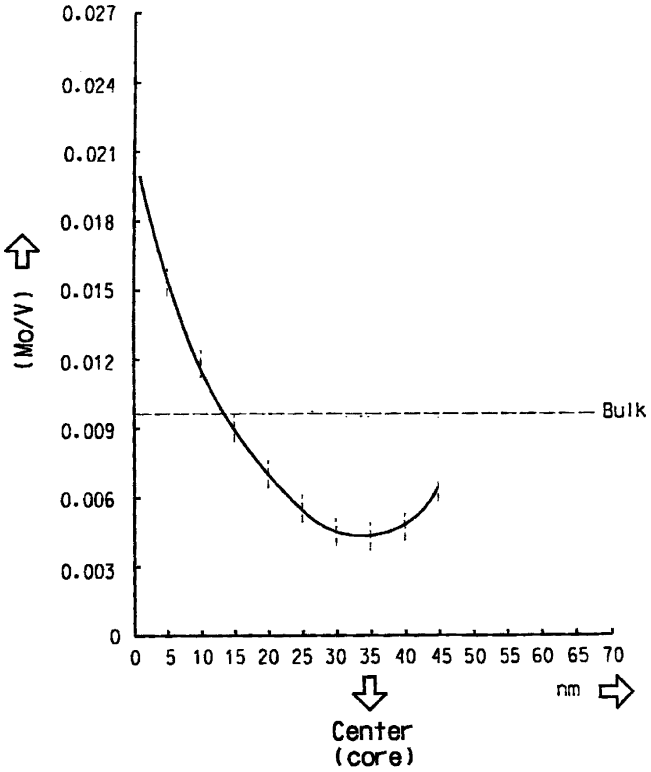

Fig. 7. Compositional depth profile of Mo/V of the grafted 1 mol% (Bi,Mo)VPO is shown in plot A, confirming surface enrichment of Mo. Data from the co-precipitated catalyst (bulk) are shown in B.

$Bi_{0.05}$ $Mo_{0.05}$ $O)_2P_2O_{7-\delta/2}$, anion vacancies resulting from the substitution of Bi^{3+} in V^{4+} are countered by the higher valent cation Mo^{6+}, with the net effect of optimizing the anion defect concentration and glide defect concentration and maintaining the surface vanadium oxidation state. From the compositional profile we have observed, the Bi–Mo ratio varies from the surface into the bulk. In view of the large ionic size differences between vanadium and bismuth, it is unlikely that bismuth will be located on the vanadium

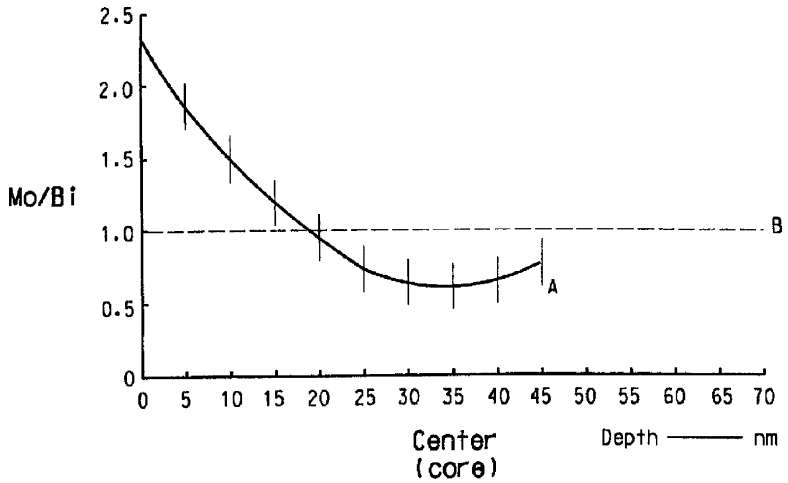

Fig. 6. Compositional depth profile of Mo/Bi ratios (scaled) plotted as a function of depth in the catalyst from the surface to the interior (core) of cross-sectioned samples. Plot A is for grafted 1 mol% (Bi,Mo)VPO catalyst and plot B is for co-precipitated catalyst prepared by co-precipitation of promoter cations with the precursor. The grafted catalysts show surface enrichment of Mo and the core enrichment of Bi. Statistical variations are shown. The co-precipitated catalyst (B) does not show this behavior. We have estimated the promoter concentrations from the surface and the bulk of the catalyst using standards. It may be noted that the data are derived uniquely, from localized regions of the sample which contains small catalyst particles. This information is difficult to obtain from other molecular diffraction methods (especially when particle sizes are quite small), as they tend to average information from a large area of sample.

sites in the vanadyl pyrophosphate structure, except in compositional regions largely depleted of bismuth, which are near the surface of the catalyst. The compositional gradient profile and the importance of the formation of a surface region depleted of some bismuth is further supported by the observation that catalysts prepared by co-precipitating the promoter cations with the vanadium phosphate precursor during precursor synthesis do not show a similar enrichment of Mo on the catalyst surface. Those systems exhibit smaller performance improvements, as a function of promoter level, than is observed for the supported catalyst systems. For those systems, the largest activity gains require higher levels of promoter cations and are accompanied by some loss in selectivity to maleic anhydride.

Co-precipitated catalyst systems are described here for comparison with the supported promoter synthetic method described earlier. Our investigations of the systems have also shown a mixture of some minor phases, namely, VPO containing only Mo, Bi–VPO compounds and undoped VPO crystals. Mo–VPO crystals exhibited defective structures. $BiPO_4$, Bi_5PO_{10} type and Mo-oxide phases have so far not been detected in our study. In general, the co-precipitated systems exhibit smaller performance improvements, as a function of promoter level, than is observed for the grafted catalyst systems. For those systems, the largest activity gains require higher levels of promoter cations and are accompanied by some loss in selectivity to maleic anhydride. Morphologies of the surface and in the interior of the particles were also examined in the cross-sectioned samples. This catalyst composition is different from the calcined and activated (Bi,Mo)-promoted VPO catalysts prepared by the co-precipitated method which did not show compositional depth profile, with Mo/Bi ratio of approximately 1 (Fig. 6, plot B).

4. Conclusions

In summary, our novel findings indicate elevated levels of Mo in the catalyst surface layers, and we believe that this improved microstructure is related to the enhanced catalytic performance. These surface compositional findings of the promoted catalyst and the synthetic procedures are novel and provide important insights into the surface microstructure and the unusual composition of the catalyst.

5. Future challenges

The oxidation of *n*-butane to maleic anhydride is a remarkably selective fourteen electron oxidation. To date, vanadium phosphorus oxide based catalysts are still the most active and selective system for this chemistry. It is likely however, that other, highly active and selective catalysts exist with perhaps different properties (stability, lattice oxygen capacity). However, to date none have been discovered. Significant progress in the area can be made when the nature of the surface and surface species of VPO catalysts with several other promoters is elucidated under in situ conditions. By understanding the nature of active species, more active catalysts (e.g. those having higher surface areas, or placed on high surface area supports) and perhaps more stable catalysts could be developed. Steps towards this goal have been realized by in situ microscopy studies, as described in this paper, and in situ EXAFS studies. For VPO chemistry, a second major challenge is to understand the role of the nature of the equilibrated catalyst and the role played by activation conditions on generating the final, equilibrated catalyst, and the effect of catalyst compositional changes on the catalyst activation. Large, parallel microreactor systems are probably best suited to investigating this very large parameter space. Here too, in situ studies can have an important role to play to advance the field. In this paper, we have discussed the nature of anion vacancies, especially near the catalyst surface, and the marked effect on performance which was observed. These vacancy structures may also be induced and perhaps stabilized by investigating catalyst/support interactions. These approaches may be crucial to creating even more active catalysts, with higher productivities for this chemistry and for other selective oxidations. Finally, we speculate that the stabilization of furan intermediate in the butane oxidation and its subsequent hydrogenation to THF (or THF in a single step) by overcoming the thermodynamically favorable MA production, can have a huge economic impact.

Acknowledgements

Pratibha L. Gai thanks Prof. G.J. Hutchings for the kind invitation to prepare the manuscript. We thank L.G. Hanna, F. Gooding and L. Wang of DuPont (CRD) for technical support.

References

[1] G. Centi, Catal. Today 16 (1993) 1.
[2] P.L. Gai, K. Kourtakis, Science 267 (1995) 661.
[3] G.J. Hutchings, et al., Catal. Today 33 (1997) 161.
[4] E. Bordes, Catal. Today 16 (1993) 27.
[5] P.L. Gai, Acta. Cryst. B53 (1997) 346.
[6] P.L. Gai, K. Kourtakis, R. Coulson, Jacobsen, J. Phys. Chem. 101 (1997) 9916.
[7] P.L. Gai, Topics Catal. 8 (1999) 91.
[8] P.L. Gai, Topics Catal. 21 (2002) 161.
[9] P.L. Gai, E.D. Boyes, Electron Microscopy in Heterogeneous Catalysis, Institute of Physics, UK, 2003.
[10] M.T. Sananes, G.J. Hutchings, J. Volta, J. Catal. 154 (1995) 253.
[11] G.J. Hutchings, Appl. Catal. 72 (1991) 1.
[12] J. Haber, V. Zazhigalov, J. Stoch, L. Bogutskaya, I. Batcherikova, Catal. Today 33 (1997) 39.
[13] S. Irusta, A. Boix, B. Pierini, C. Caspani, J. Petunchi, J. Catal. 187 (1999) 298.
[14] G.J. Hutchings, R. Higgins, J. Catal. 162 (1996) 153.
[15] Y. Gorbonova, Linde, Dockl. USSR, 245 (1979) 584.

[16] K. Kourtakis, et al., US 4,442,226.
[17] E.D. Boyes, P.L. Gai, Ultramicroscopy 67 (1997) 219.
[18] P.L. Gai, Adv. Mater. 10 (1998) 1251.
[19] E.D. Boyes, Adv. Mater. 10 (1998) 1277.
[20] J. Haggin, C&E News, Am. Chem. Soc. 73 (1995) 39.
[21] M. Jacoby, C&E News, Am. Chem. Soc. 80 (2002) 26.
[22] K. Kourtakis, P.L. Gai, Vanadium-phosphorus oxide catalysts with promoter reagents, WO 2001 052983 20010726.
[23] P.B. Hirsch, et al., Electron Microscopy of Thin Crystals, Krieger, NY, 1977.